

# Extraction of Left Ventricular Contours From Left Ventriculograms by Means of a Neural Edge Detector

Kenji Suzuki\*, *Member, IEEE*, Isao Horiba, Noboru Sugie, *Member, IEEE*, and Michio Nanki

**Abstract**—We propose a method for extracting the left ventricular (LV) contours from left ventriculograms by means of a neural edge detector (NED) in order to extract the contours which accord with those traced by a cardiologist. The NED is a supervised edge detector based on a modified multilayer neural network, and is trained by use of a modified back-propagation algorithm. The NED can acquire the function of a desired edge detector through training with a set of input images and the desired edges obtained from the contours traced by a cardiologist. The proposed contour-extraction method consists of 1) detection of “subjective edges” by use of the NED; 2) extraction of rough contours by use of low-pass filtering and edge enhancement; and 3) a contour-tracing method based on the contour candidates synthesized from the edges detected by the NED and the rough contours. Through experiments, it was shown that the proposed method was able to extract the contours in agreement with those traced by an experienced cardiologist, i.e., we achieved an average contour error of 6.2% for left ventriculograms at end-diastole and an average difference between the ejection fractions obtained from the manually traced contours and those obtained from the computer-extracted contours of 4.1%.

**Index Terms**—Contour extraction, neural network, subtle edge, supervised edge detection.

## I. INTRODUCTION

**E**XTRACTION of left ventricular (LV) contours (borders) from left ventriculograms is the most fundamental task in the assessment of cardiac functions of the heart such as LV volume, and ejection fraction. Accordingly, many investigators have developed a number of methods for the automated extraction of the contours from left ventriculograms [1]–[8]. In left ventriculograms, the density within the left ventricle is not uniform because of the following: contrast medium in the left ventricle may be diluted with blood from the mitral valve; it is not possible to use a large amount of contrast medium without increasing the risk for the patient. Therefore, most edges of the LV contours are subtle, i.e., they are not clear edges with uniform contrast (such edges are referred to as “subtle edges” in this paper).

Manuscript received January 31, 2002; revised December 9, 2003. This work was supported in part by the Ministry of Education, Science, Sports and Culture of Japan under a grant-in-aid for a quantum information theoretical approach to life science and a grant-in-aid for encouragement of young scientists. The Associate Editor responsible for coordinating the review of this paper and recommending its publication was J. Duncan. *Asterisk indicates corresponding author.*

\*K. Suzuki is with the Kurt Rossmann Laboratories for Radiologic Image Research, the Department of Radiology, The University of Chicago, 5841 S. Maryland Ave., Chicago, IL 60637 USA (e-mail: suzuki@uchicago.edu).

I. Horiba is with the Faculty of Information Science and Technology, Aichi Prefectural University, Aichi 480-1198, Japan.

N. Sugie is with the Faculty of Science and Technology, Meijo University, Nagoya 468-8502, Japan.

M. Nanki is with Chubu Rosai Hospital, Nagoya 455-8530, Japan.

Digital Object Identifier 10.1109/TMI.2004.824238

In clinical applications, a cardiologist may manually modify some parts of the LV contours extracted by an automated method, with which he/she does not agree. Therefore, the development of a method for extracting the LV contours in agreement with the cardiologist’s decision is needed by cardiologists. Our purpose in this study was to develop a method for extracting the LV contours that accord with the cardiologist’s decision.

Various methods for extracting LV contours have been developed for X-ray images [1]–[8], ultrasonic images [9]–[15], computed tomography (CT) images or MRIs [16]–[21], and emission CT images [22]–[24]. Most methods consisted of detection of edges (or boundaries) and integration of these as a contour. The detection of edges was performed by use of an edge detector or a thresholding technique. The integration of edges was performed by use of a searching technique or a deformable contour model such as the Snakes [25]. Therefore, the performance of contour extraction in terms of agreement with the contours traced by a cardiologist would depend on the performance of the edge detection method.

In the field of computer vision, many edge detectors have been proposed [26]–[32]. These edge detectors could detect edges effectively from various kinds of images, including medical images such as left ventriculograms [3], [4], echocardiograms [9], [13], cardiac CT [16], cardiac MRI [17], or nuclear images [22]. However, the conventional edge detectors cannot detect the “subjective edges” that are judged when a person tries to trace the contour of an object in an image, e.g., the LV contour traced by a cardiologist. The subjective edges can differ when different persons trace them. Therefore, the detected edges would not necessarily accord with the contours traced by a certain cardiologist, because they do not have the function of training, i.e., the edges are determined by certain criteria (or a definite model) in these edge detectors.

Recently, in the field of signal processing, nonlinear filters based on a multilayer neural network (NN), called neural filters, have been studied [33]–[42]. Suzuki *et al.* have developed training methods [38], [39], design methods [36], [40], and an analysis method [42] for neural filters, and applied them for reduction of the quantum mottle in radiologic images [37], [41]. The neural filters can acquire the function of the desired filter by training with a set of input images and the desired images.

In this paper, we extend the use of neural filters and propose a supervised edge detector, called a neural edge detector (NED), for detecting the subjective edges, and develop a method for extracting LV contours from left ventriculograms by means of the NED in order to extract the contours that agree with those traced by a cardiologist. We evaluated the effectiveness of the proposed method in extracting the LV contours in comparison to those traced by an experienced cardiologist.

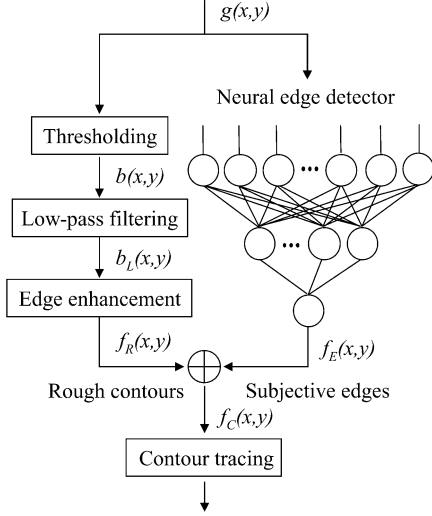


Fig. 1. Method for extracting LV contours from left ventriculograms by means of the NED.

## II. PREVIOUS WORK

Edge detectors based on various NN models can be classified into the following four broad classes.

- 1) Edge detectors based on cellular NNs [43]–[45].
- 2) Edge detectors based on self-organizing maps [46]–[48].
- 3) Edge detectors based on Hopfield networks [49]–[51].
- 4) Edge detectors based on multilayer NNs [52]–[54].

Because the above edge detectors except those in class 4 are unsupervised ones, they cannot necessarily detect the subjective edges detected by a cardiologist. As for the edge detectors in class 4, since the NNs are used as a classifier that classifies directly whether a certain pixel belongs to the class, an edge or the background, they cannot handle continuous values such as edge magnitude and the fluctuation of a cardiologist's tracing. The capability of handling the edge magnitude is important for extracting the subjective edges including the cardiologist's fluctuation from subtle edges, because it is difficult for NN-based edge detectors to learn various edges having different gradients and widths as a uniform thin edge where the width is one pixel.

## III. CONTOUR-EXTRACTION METHOD

A block diagram of the proposed contour-extraction method is shown in Fig. 1. The proposed method consists of 1) detection of the subjective edges by use of the NED, 2) extraction of rough contours by use of low-pass filtering and edge enhancement, and 3) a contour-tracing method based on the contour candidates that are synthesized from the edges detected by the NED and the rough contours. The subjective edges detected by the NED play a major role in contour extraction in making the contours approach those traced by a cardiologist; the rough contours play a supporting role for tracing the target contours stably. We describe each part of the method below.

### A. Edge Detection by Use of the Neural Edge Detector

1) *Architecture of the Neural Edge Detector:* We are extending the neural filters [37]–[42] to deal with the detection of the subjective edges detected by a cardiologist, and we call this technique NED. The architecture of the NED is shown in

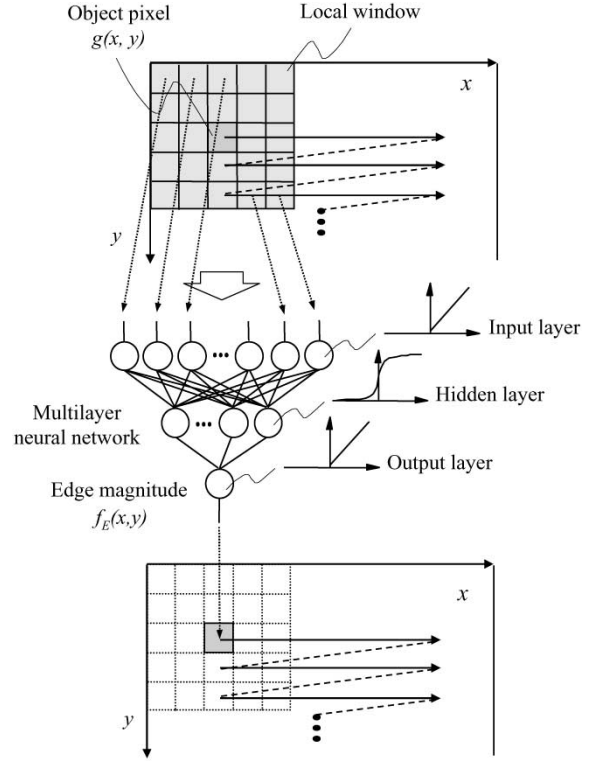


Fig. 2. Architecture of the NED.

Fig. 2. The NED consists of a modified multilayer NN, which can directly handle input gray levels and the output edge magnitude. The structure of a multilayer NN is modified to handle the edge magnitude. The modified multilayer NN employs an identity function instead of a sigmoid function as the activation function of the unit in the output layer because the characteristics of an NN were significantly improved with a linear function when applied to the continuous mapping of values in image processing [55], [56], for example (see Appendix for theoretical considerations). In the NED, edge detection is performed by scanning of an input image with the modified multilayer NN in which the activation functions of the units in the input, hidden, and output layers are an identity, a sigmoid, and an identity function, respectively.

The pixel values of an original left ventriculogram are normalized first. The pixel values within a local window  $R_S$  are input to the NED: the inputs to the NED are a normalized pixel value  $g(x, y)$  of an original input image and spatially adjacent normalized pixel values. The output of the NED is a continuous value, which corresponds to the center pixel in the local window, represented by

$$f_E(x, y) = G_M \cdot \text{NN}(\mathbf{I}_{x,y}) \quad (1)$$

where

$$\mathbf{I}_{x,y} = \{g(x - i, y - j) / G_M \mid i, j \in R_S\} \quad (2)$$

is the input vector to the NED,  $f_E(x, y)$  is an estimate for the desired edge magnitude,  $x$  and  $y$  are the indices of coordinates,  $\text{NN}(\cdot)$  is the output of the modified multilayer NN,  $g(x, y)$  is a normalized pixel value,  $G_M$  is a normalization factor for normalizing gray levels such that the maximum level of the gray scale is one and the minimum level is zero, and  $R_S$  is the local window of the modified multilayer NN.

All pixels in an image may be entered as the inputs to the NED by scanning of the entire image with the NED. The NED can be designed by training such that the input images are converted to the desired edge images. The property of a multilayer NN for universal approximation [57], [58] guarantees capability of the NED, i.e., because it has been shown theoretically that a multilayer NN can realize any continuous mapping (including any continuous functions) approximately, the NED would have a high performance.

2) *Synthesizing the Teacher Images:* The teacher image containing the desired edges is synthesized from the contour that was traced by a cardiologist. The contour traced by a cardiologist may include the fluctuation of the cardiologist's tracing. It might be difficult for the NED to learn the contour including the fluctuation as a thin curve. Therefore, the teacher image is synthesized by smoothing of the contour traced by a cardiologist with a Gaussian filter to improve the convergence of the training as follows:

$$T_C(x, y) = C_D(x, y) * G(x, y; \sigma) \quad (3)$$

where  $C_D(x, y)$  is the image containing the contour traced by a cardiologist,  $G(x, y; \sigma)$  is a Gaussian function with standard deviation  $\sigma$ , and  $*$  is the convolution operator. Note that  $C_D(x, y)$  is one at the coordinates of the contour traced by a cardiologist, and zero at others.  $G(x, y; \sigma)$  is normalized such that the area under the Gaussian function is one.

3) *Training of the Neural Edge Detector:* In order to learn the relationship between the input image and the desired edges, the NED is trained with a set of input images and the teacher images by a change in the weights between the layers. The error to be minimized by training is defined by

$$E = \frac{1}{2P} \sum_p (T_C^p - f_E^p / G_M)^2 \quad (4)$$

where  $p$  is a training pixel number,  $T_C^p$  is the  $p$ th training pixel in the training regions in the teacher images,  $f_E^p$  is the  $p$ th training pixel in the training regions in the output images, and  $P$  is the number of training pixels (which corresponds to the number of pixels in the training regions). The NED is trained by the modified back-propagation (BP) algorithm [55], which was derived for the structure described above, i.e., an identity function is employed as the activation function of the unit in the output layer, in the same way as the standard BP algorithm [59], [60]. The characteristics of training were improved with the modified BP algorithm in the application to the continuous mapping issues [55], [56] (see Appendix for theoretical considerations). In the modified BP algorithm, the correction of the weight between the  $m$ th unit in the hidden layer and the unit in the output layer is represented by

$$\Delta W_m^O = -\eta \cdot \delta \cdot O_m^H = -\eta(T_C - f_E / G_M) O_m^H \quad (5)$$

where  $\eta$  is the learning rate,  $O_m^H$  is the output of the  $m$ th unit in the hidden layer, and  $\delta$  is the delta of the delta rule [59], [60]. By use of the delta, the corrections of any weights can be derived in the same way as the BP algorithm. The training would be performed until the error  $E$  becomes less than or equal to the predetermined error, or the number of training epochs exceeds the predetermined number.

## B. Extraction of Rough Contours

For extraction of rough contours, the following three processes are performed on the original left ventriculograms.

1) *Thresholding:* The original left ventriculogram  $g(x, y)$  is converted into a binary image by use of a thresholding technique based on Otsu's threshold selection [61] as follows:

$$b(x, y) = \begin{cases} G_M, & \text{if } g(x, y) \geq t_h \\ 0, & \text{if } g(x, y) < t_h \end{cases} \quad (6)$$

where  $t_h$  is the threshold that is determined by Otsu's threshold selection. Otsu's threshold selection is a technique for determining a threshold from a histogram. This method selects the lowest point between two classes in the histogram automatically (it is formulated as discriminant analysis). A particular criterion function is used as a measure of statistical separation, i.e., the method involves minimizing the ratios of between-class variance to the total variance.

2) *Low-Pass Filtering:* Low-pass filtering with a Hamming window [62] is performed on the binary image  $b(x, y)$  as follows:

$$b_L(x, y) = \mathfrak{S}^{-1}[\mathfrak{S}\{b(x, y)\} \cdot H(R_H)] \quad (7)$$

where  $\mathfrak{S}(\cdot)$  and  $\mathfrak{S}^{-1}(\cdot)$  are the Fourier transform operator and the inverse Fourier transform operator, respectively, and  $H(R_H)$  is a Hamming window function with a diameter  $R_H$ .

3) *Edge Enhancement:* The rough contours are obtained by performing an edge-enhancement technique on the low-pass-filtered image  $b_L(x, y)$  as follows:

$$f_R(x, y) = \psi\{b_L(x, y)\} \quad (8)$$

where  $\psi(\cdot)$  is the Sobel operator [26].

## C. Contour-Tracing Method

Contour candidates are obtained by synthesizing of the edges detected by the NED and the rough contours, as described below:

$$f_C(x, y) = W_W \cdot f_R(x, y) + (1 - W_W) f_E(x, y) \quad (9)$$

where  $W_W$  is a weighting factor. We modified a method for tracing coronary arteries in [55], and we use it as a contour-tracing method. First, we assign two points, which are the ends of the contour to be traced, manually to the contour-tracing method. With the contour-tracing method, an LV contour is traced from one given point to the other point on the contour-candidate image. Let  $\mathbf{r}$  be the vector radiating in all directions from a certain object point  $P$ . An average pixel value on the vector in direction  $\theta$  is calculated by the following equation:

$$g_S(\theta) = \frac{\sum_{x, y \in R_{P, \theta}} f_C(x, y)}{|\mathbf{r}|} \quad (10)$$

where  $R_{P, \theta}$  is a group of the coordinates on the vector in direction  $\theta$  from the current object point  $P$ , and  $|\mathbf{r}|$  is the length of the vector  $\mathbf{r}$ . The average pixel value on the vector is weighted by a weighting function, as follows:

$$g_C(\theta) = g_S(\theta) \cdot w_f(\theta - D) \quad (11)$$

where  $D$  is the previous tracing direction,  $w_f(\theta - D)$  is a weighting function represented by

$$w_f(\theta - D) = 1 - \left( \frac{\theta - D}{w_D \pi} \right)^2 \quad (12)$$

and  $w_D$  is a weighting parameter for determining the search range. The next tracing direction  $D_N$  is determined by

$$D_N = \arg \max \{g_C(\theta)\} (D - w_D \pi \leq \theta \leq D + w_D \pi). \quad (13)$$

Thus, the next object point  $P_N$  is determined as the end of the vector in the tracing direction  $D_N$ . By treating  $P_N$  and  $D_N$  as the current object point  $P$  and the previous tracing direction  $D$ , the tracing process proceeds. These processes are performed repeatedly until the following stopping condition is fulfilled:  $g_S(D_N)$  is less than 5% of  $G_M$ . The 5% is a margin for preventing a wrong tracing due to noise, and was determined empirically. The tracing for one contour is performed twice from the given two points. The contour from one point to the other is obtained by combining the two traced curves at their crossing point.

#### IV. EVALUATION OF THE PERFORMANCE OF THE NED

We carried out experiments to compare the performance of the NED with that of a conventional edge detector.

##### A. Training the NED

In this study, we used twelve left ventriculograms at end-diastole (size:  $512 \times 512$  pixels, gray scale: 1 024 levels) and twelve left ventriculograms at end-systole, which had been acquired from twelve patients with a digital angiography system (DFA-100, Hitachi Medical, Tokyo, Japan) in a hospital. The normalization factor  $G_M$  was set to be the maximum level of the gray scale (1 023). We applied a digital subtraction angiography (DSA) technique to the left ventriculograms. The DSA technique (temporal subtraction) involves subtracting the image obtained without a contrast medium from an image taken with a contrast medium. By use of the DSA technique, we obtained the left ventriculogram that visualizes the left ventricle without interference from surrounding structures such as the ribs. Examples of the images used for training the NED are shown in Fig. 3. Fig. 3(a) and (c) shows a left ventriculogram at end-diastole in the  $30^\circ$  right anterior oblique projection (a region of  $340 \times 340$  pixels is displayed as an example) and a left ventriculogram at end-systole (from a different patient), respectively. It should be noted that some parts of the contours of the left ventricles are very subtle. An experienced cardiologist (M.N.; 25 years of experience) traced the left ventricles in the left ventriculograms very carefully. He traced the contour by viewing the images before and after the current image. He traced and modified the contour alternately until he was satisfied with the result. We used the contours traced in this way as a “gold standard.” The teacher images shown in Fig. 3(b) and (d) were synthesized from the contours traced by the cardiologist on the basis of (3), where  $\sigma$  was 1.25 pixels, which corresponded to the reproducibility of a cardiologist’s tracing in a controlled situation [63].

The training of the NED for left ventriculograms at end-diastole and that for left ventriculograms at end-systole were performed separately, because the edges of the contours in the two left ventriculograms seemed to be different. We trained the NED

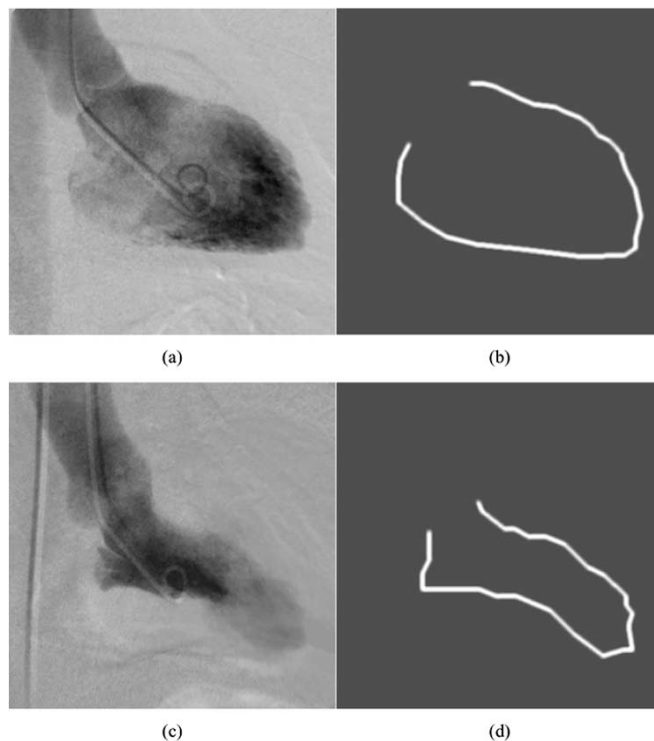


Fig. 3. Examples of the images used for training the NED. (a) Left ventriculogram at end-diastole used as the input image. (b) Teacher image containing the desired edges for the left ventriculogram (a), which was synthesized from the contour traced by an experienced cardiologist. (c) Left ventriculogram at end-systole used as the input image. (d) Teacher image for the left ventriculogram (c).

for left ventriculograms at end-diastole with a set of the input image and the teacher image shown in Fig. 3(a) and (b). The training region was selected to be the region that covered the desired edges in the teacher image. A three-layer structure was employed as the structure of the NED, because any continuous mapping (including any continuous functions) can be realized approximately by three-layer NNs [57], [58]. The local window of the NED was selected to be eleven by eleven pixels. The number of units in the hidden layer was 20. Thus, the numbers of units in the input, hidden, and output layers were 121, 20, and one, respectively.

With the parameters above, the training of the NED was performed on 200 000 epochs—one epoch means one training run for one training set—and converged with a mean absolute training error (MATE) between the input image and the teacher image of 19.9%. The CPU execution time for the training was 126 hours on a workstation (UltraSPARC-II 300 MHz, Sun Microsystems). After training, a method for designing the optimal structure of an NN [64] was applied to the trained NED. The method is a sensitivity-based pruning method, i.e., the sensitivity to the training error was calculated when a certain unit was removed virtually, and the unit with the minimum training error was removed first. The redundant units in the input and hidden layers were removed on the basis of the effect of removing each unit on the training error, and then the NED was retrained to recover the potential loss due to the removal. Each process was performed alternately, resulting in a reduced structure where redundant units were removed. As a result, the optimal number of units in the input layer and that in the hidden

layer were determined as 64 (within a nine-by-nine-pixel region) and ten, respectively. Similarly, we trained the NED for left ventriculograms at end-systole with a set of the input image and the teacher image shown in Fig. 3(c) and (d). The training converged with an MATE of 21.9%. The optimal number of units in the input layer and that in the hidden layer were 70 (within a nine-by-nine-pixel region) and nine, respectively.

It should be noted that the training of the NED could not converge when we did not use the Gaussian filtered contour, but directly used the contour traced by a cardiologist as the teacher image. This is because training the contour containing the fluctuation to be the contour containing no fluctuation was difficult for the NED. This result indicates that the use of the teacher images synthesized in consideration of the fluctuation is important for training the NED.

### B. Comparison With a Conventional Edge Detector

A well-known representative of conventional edge detectors is the Marr-Hildreth edge detector [28], which has been used in a method for extracting LV contours in left ventriculograms [4]. For comparison of the NED with the Marr-Hildreth edge detector, the parameters of the Marr-Hildreth edge detector were optimized with the images used for training the NED under the minimum-mean-square error criterion, defined by (4). Thus, the Marr-Hildreth edge detector had the highest performance for the training images. The results of edge detection are shown in Fig. 4. The Marr-Hildreth edge detector failed to detect subtle edges. The edges detected by the Marr-Hildreth edge detector are discontinuous, i.e., some parts of the edges near the target contour are missing. Furthermore, these edges are different from the desired edges in the teacher image (i.e., the contour traced by a cardiologist). On the basis of such edges, even a better contour-tracing method may not be able to trace the contour well. In contrast, in the edges detected by the trained NED, there is little noise near the target contour. The detected edges are relatively continuous and are similar to the desired ones.

### C. Quantitative Evaluation With Nontraining Images

We used fourfold cross-validation [65] for evaluation of edge detectors. This cross-validation involves four separate runs on four sets of test samples. First, twelve left ventriculograms at end-diastole or at end-systole were partitioned into four different portions, each of which included three left ventriculograms. In each of the four runs, one portion was used for training the NED, and the remaining three portions were pooled for testing. Thus, the number of NEDs to be trained for left ventriculograms at end-diastole or at end-systole, the number of training images for each NED, and the number of test (nontraining) images for each NED were four (eight in total), three (24 in total), and nine (72 in total), respectively. The training of each NED was performed on 200 000 epochs, and each training converged with MATEs of 17.7%–22.5%. We applied the method for designing the optimal structure of an NN [64] for design of the trained NEDs. As a result, the numbers of the units in the input layer and the numbers of the units in the hidden layer were 65–81 and 6–12, respectively. The parameters of the Marr-Hildreth edge detector were optimized in the same way as described in the previous subsection; thus, the Marr-Hildreth edge detector had the highest performance.

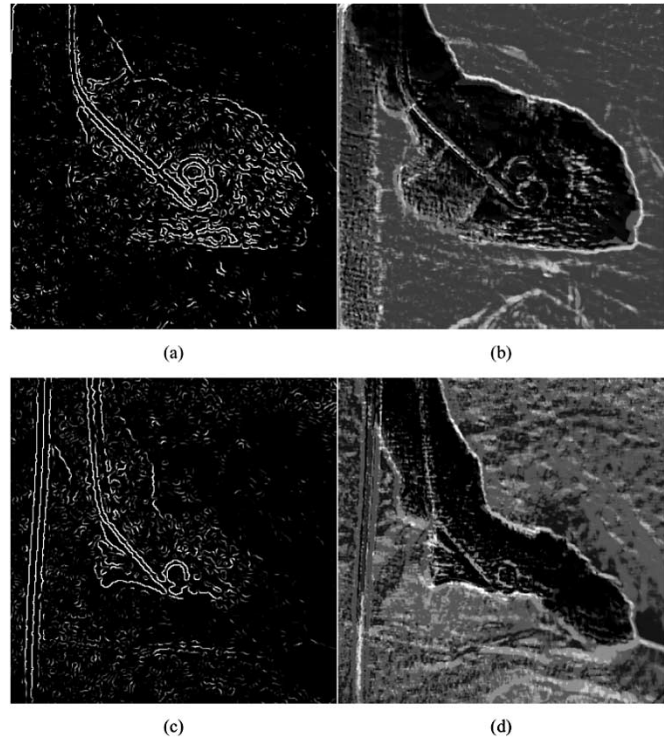


Fig. 4. Comparison of the edges detected by the trained NED with those detected by a conventional edge detector. (a) Output image of the Marr-Hildreth edge detector, the parameters of which were optimized with the images used for training the NED, for the left ventriculogram shown in Fig. 3(a). (b) Output image of the trained NED. (c) Output image of the Marr-Hildreth edge detector for the left ventriculogram shown in Fig. 3(c). (d) Output image of the trained NED.

TABLE I  
COMPARISON OF THE PERFORMANCE OF THE NED WITH THAT OF A CONVENTIONAL EDGE DETECTOR FOR NONTRAINING IMAGES

MAE	OMHED	NED
Min.	0.37	0.26
Ave.	0.41	0.30
Max.	0.47	0.39

MAE: Mean absolute error,  
OMHED: Optimized Marr-Hildreth edge detector,  
NED: Neural edge detector.

The mean absolute error (MAE) between the detected edges and the desired edges synthesized from the contour traced by a cardiologist (i.e., the same as the teacher image) for 72 test (nontraining) images is shown in Table I. The MAEs of the NED were smaller than those of the Marr-Hildreth edge detector. This result demonstrates that the performance of the NED is higher in terms of detection of the subjective edges detected by a cardiologist.

## V. EVALUATION OF THE PERFORMANCE OF THE CONTOUR-EXTRACTION METHOD

### A. Results of Contour Extraction

The method for extracting the rough contours was applied to left ventriculograms. The parameter of the low-pass filtering  $R_H$  was determined as  $Nq/5$  such that the target contour was covered with the rough contours sufficiently ( $Nq$  is the Nyquist frequency). The result of the extraction of rough contours for the

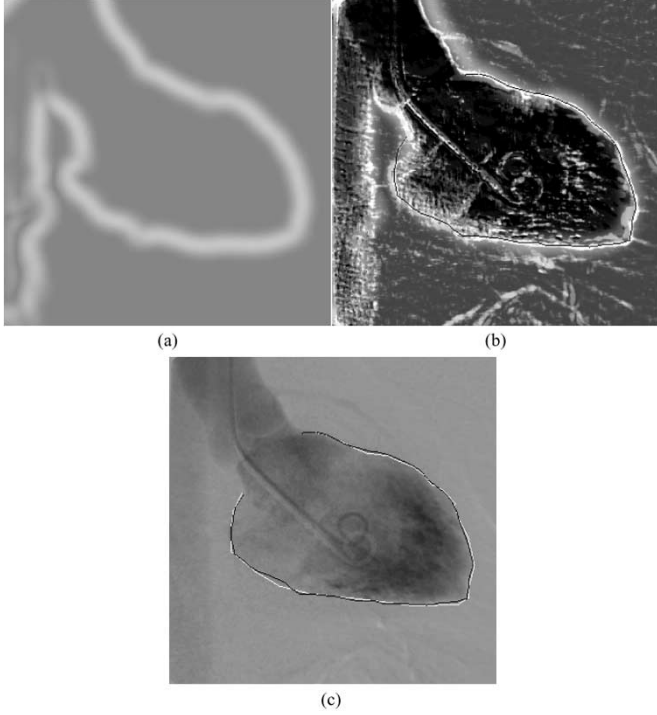


Fig. 5. Result of the extraction of the LV contour. (a) Rough contours extracted by the rough-contour-extraction method. (b) Image of the contour candidates, which is overlaid with the result of the contour tracing. (c) Comparison of the contour extracted by the proposed method, indicated by a black curve, with that traced by an experienced cardiologist, indicated by a white curve ( $E_C = 1.6\%$ ).

left ventriculogram shown in Fig. 3(a) is shown in Fig. 5(a). The contour candidates were synthesized from the rough contours and the edges detected by the trained NED. We used a weighting factor  $W_W$  of 0.5. The image of the contour candidates is shown in Fig. 5(b). We assigned two points for tracing to the contour-tracing method. These two points were near the mitral valve-aortic root junction and the junction of the aortic root and the anterior endocardium. The reproducibility of determination of the two points would be similar to that of a cardiologist's tracing [63], which corresponded to a standard deviation of 1.25 pixels, because the two points are generally included in the contour traced by a cardiologist.

Next, the contour-tracing method was applied to the contour candidates. The parameters of the contour-tracing method,  $|r|$  and  $W_D$ , were determined empirically as 15 pixels and 0.35, respectively. By use of the contour-tracing method, the contour was traced stably, as shown in Fig. 5(b). Fig. 5(c) shows the contour extracted by the proposed method, overlaid with the target contour traced by a cardiologist. These two contours agree extremely well.

### B. Quantitative Evaluation

For evaluation of the performance of the proposed method, the contour was closed by connecting the given two points, and then the following regions were calculated:

$$a_P(x, y) = \begin{cases} 1, & (x, y) \in R_P \\ 0, & \text{otherwise} \end{cases} \quad (14)$$

$$a_D(x, y) = \begin{cases} 1, & (x, y) \in R_D \\ 0, & \text{otherwise} \end{cases} \quad (15)$$

TABLE II  
QUANTITATIVE EVALUATION OF THE PERFORMANCE OF THE PROPOSED METHOD IN TEST SETS COMPARED TO THE CONTOURS TRACED BY A CARDIOLOGIST

	End-diastole		End-systole		$E_{FD}$ [%]
	$E_C$ [%]	$E_A$ [%]	$E_C$ [%]	$E_A$ [%]	
Min.	2.3	0.1	8.2	2.3	0.1
Ave.	6.2	4.2	17.1	11.6	4.1
Max.	12.2	8.5	35.6	27.5	9.9
SD	2.1	2.5	6.8	5.8	2.8

$E_C$ : Contour error,  $E_A$ : Area error,  $E_{FD}$ : Ejection fraction difference, SD: Standard deviation.

where  $R_P$  is the region within the contour extracted by the proposed method, and  $R_D$  is the region within the contour traced by a cardiologist. In order to evaluate quantitatively the difference between the contour extracted by the proposed method and that traced by a cardiologist, we defined a contour error as

$$E_C = \frac{\sum_{x,y \in R_E} \{a_P(x, y) \oplus a_D(x, y)\}}{\sum_{x,y \in R_E} a_D(x, y)} \quad (16)$$

where  $\oplus$  denotes the logical exclusive OR operator, and  $R_E$  is a region for evaluation. Because, in clinical applications, cardiologists use the area within the left ventricle for calculation of cardiac functions such as LV volume and ejection fraction, evaluation of the method with the area is also important from the clinical point of view. Therefore, we defined an area error as

$$E_A = \frac{\left| \sum_{x,y \in R_E} a_D(x, y) - \sum_{x,y \in R_E} a_P(x, y) \right|}{\sum_{x,y \in R_E} a_D(x, y)}. \quad (17)$$

A labeling algorithm [66] was applied to the binary image for calculation of the area. We also defined a difference in ejection fractions as

$$E_{FD} = |EF_D - EF_P| \quad (18)$$

where  $EF_D$  is the ejection fraction obtained from the contour traced by a cardiologist, and  $EF_P$  is the ejection fraction obtained from the contour extracted by the proposed method.

The fourfold cross-validation was applied for the evaluation of the proposed contour-extraction method in the same way as in the previous section, i.e., we used eight NEDs trained with eight different training sets, and applied eight test sets representing each of nine nontraining left ventriculograms. The results of the contour extraction for all test sets are shown in Table II. The average contour and area errors for left ventriculograms at end-diastole were small (6.2% and 4.2%, respectively). However, the errors for left ventriculograms at end-systole were relatively large (17.1% and 11.6%, respectively), because the areas of the left ventriculograms at end-systole were relatively small; the areas are a denominator in the definitions of errors in (17) and (16). This result indicates that the proposed contour-extraction method has a potential to extract the contours in agreement with those traced by a cardiologist. The standard deviation of the contour error and the area error for left ventriculograms at end-diastole was also small (2.1% and 2.5%, respectively). This result shows that the proposed method is stable.

The results of extraction of the contours with the least two errors, medium two errors, and the largest two errors for left ventriculograms at end-diastole and at end-systole in test sets are shown in Figs. 6–11. The images (b) display the contour extracted by the proposed method overlaid with that traced by

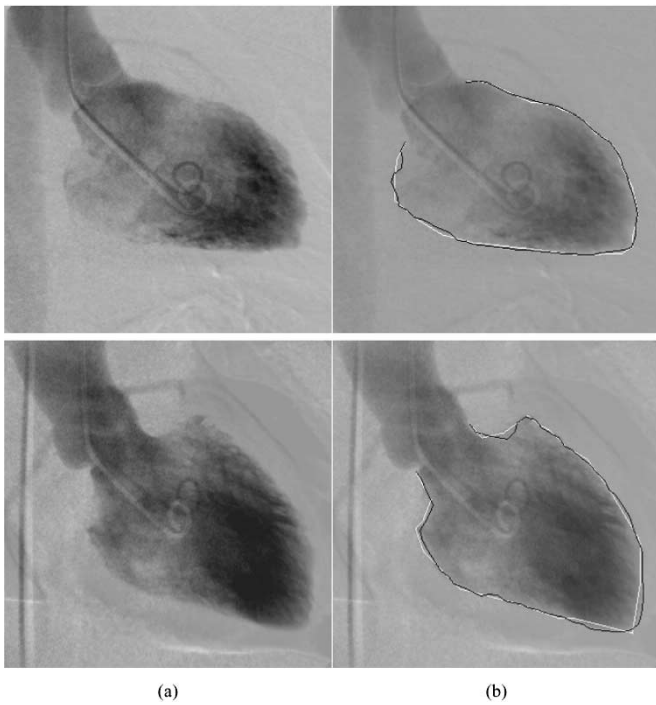


Fig. 6. Results of the contour extraction in the best two cases in test sets for left ventriculograms at end-diastole (Upper:  $E_C = 2.3\%$ ; Lower:  $E_C = 3.5\%$ ). (a) Input left ventriculogram. (b) Comparison of the contour extracted by the proposed method, indicated by a black curve, with that traced by a cardiologist, indicated by a white curve.

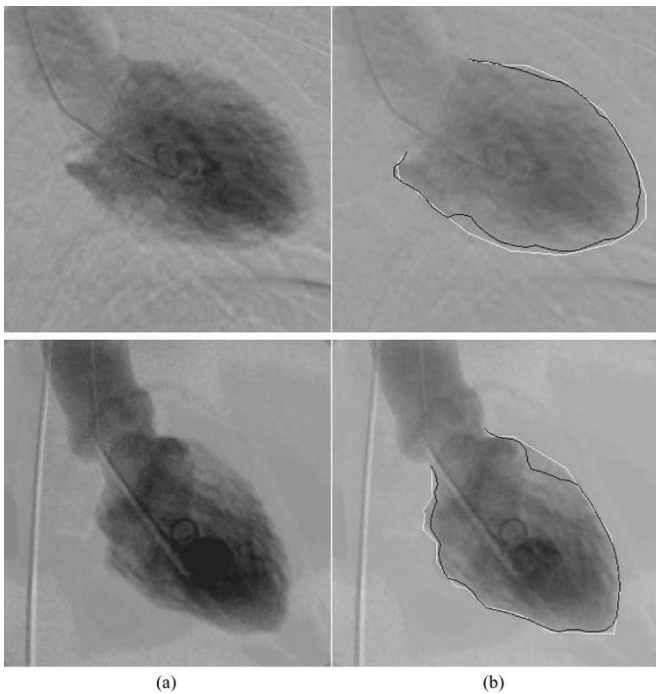


Fig. 7. Results of the contour extraction in medium two cases in test sets for left ventriculograms at end-diastole (Upper:  $E_C = 5.7\%$ ; Lower:  $E_C = 6.3\%$ ). (a) Input left ventriculogram. (b) Comparison of the contour extracted by the proposed method, indicated by a black curve, with that traced by a cardiologist, indicated by a white curve.

a cardiologist. In the best cases shown in Figs. 6(b) and 9(b), the contours extracted by the proposed method agree very well with those traced by a cardiologist. In the medium cases shown

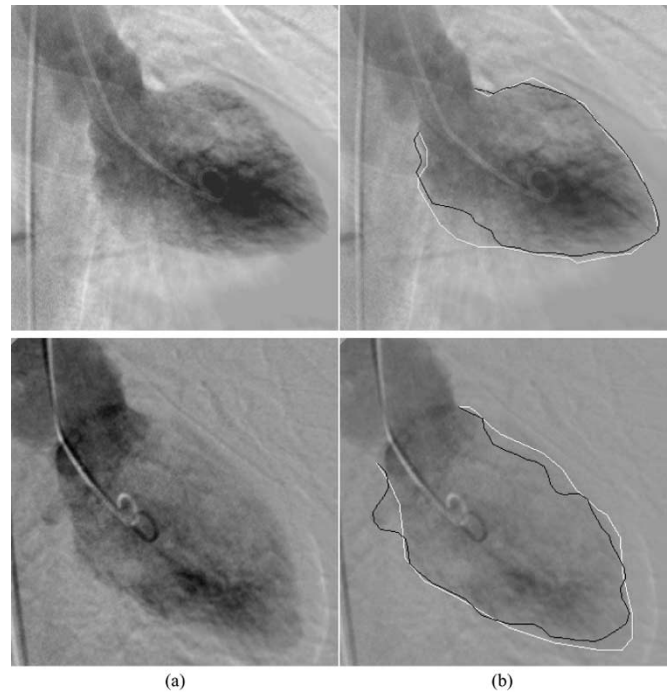


Fig. 8. Results of the contour extraction in the worst two cases in test sets for left ventriculograms at end-diastole (Upper:  $E_C = 8.7\%$ ; Lower:  $E_C = 12.2\%$ ). (a) Input left ventriculogram. (b) Comparison of the contour extracted by the proposed method, indicated by a black curve, with that traced by a cardiologist, indicated by a white curve.

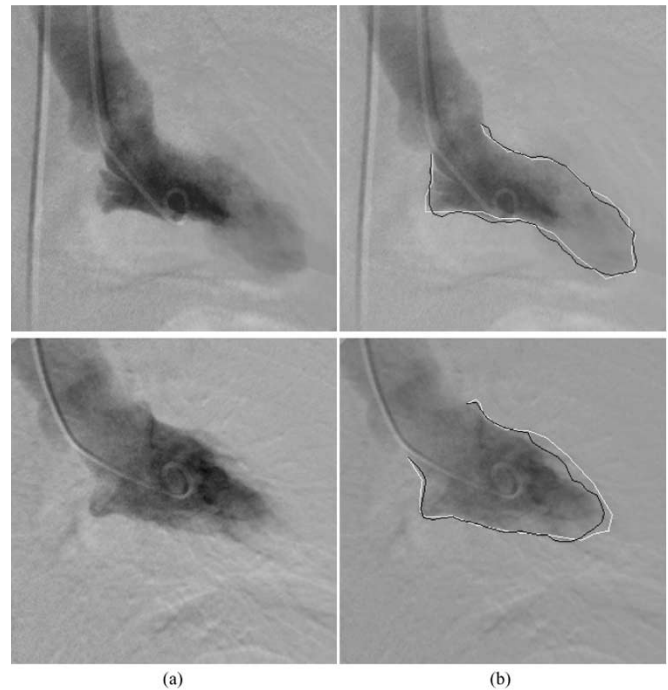


Fig. 9. Results of the contour extraction in the best two cases in test sets for left ventriculograms at end-systole (Upper:  $E_C = 8.2\%$ ; Lower:  $E_C = 9.5\%$ ). (a) Input left ventriculogram. (b) Comparison of the contour extracted by the proposed method, indicated by a black curve, with that traced by a cardiologist, indicated by a white curve.

in Figs. 7(b) and 10(b), although the proposed method failed to trace some parts due to subtle edges, the extracted contours almost agree with those traced by a cardiologist. In the worst cases shown in Figs. 8(b) and 11(b), some parts of the extracted

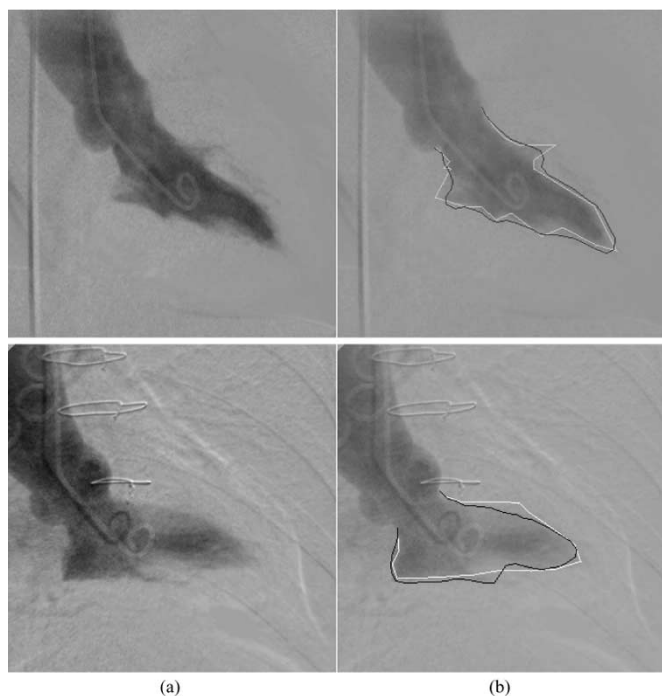


Fig. 10. Results of the contour extraction in medium two cases in test sets for left ventriculograms at end-systole (Upper:  $E_C = 13.8\%$ ; Lower:  $E_C = 14.2\%$ ). (a) Input left ventriculogram. (b) Comparison of the contour extracted by the proposed method, indicated by a black curve, with that traced by a cardiologist, indicated by a white curve.

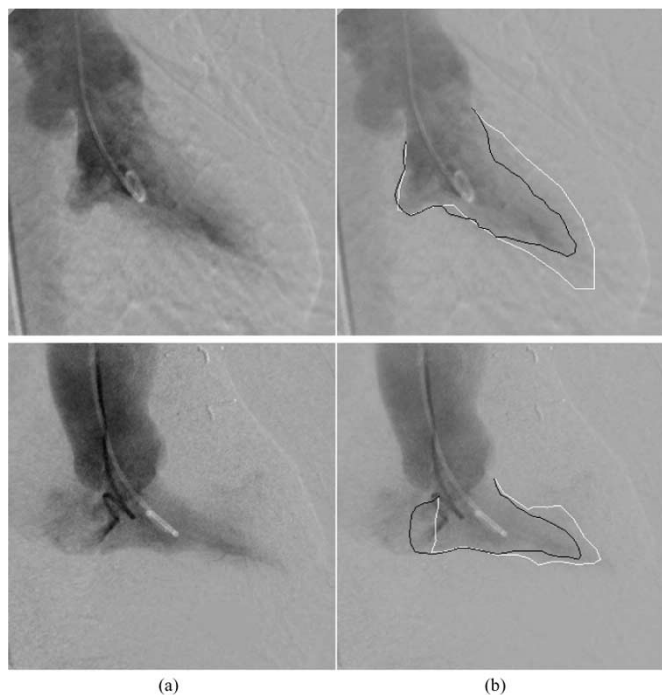


Fig. 11. Results of the contour extraction in the worst two cases in test sets for left ventriculograms at end-systole (Upper:  $E_C = 29.9\%$ ; Lower:  $E_C = 35.6\%$ ). (a) Input left ventriculogram. (b) Comparison of the contour extracted by the proposed method, indicated by a black curve, with that traced by a cardiologist, indicated by a white curve.

contours are different from the target contours because of subtle edges.

TABLE III  
PERFORMANCE OF THE PROPOSED METHOD WITHOUT THE NED

	End-diastole		End-systole		$EFD$ [%]
	$E_C$ [%]	$E_A$ [%]	$E_C$ [%]	$E_A$ [%]	
Min.	9.1	8.2	12.6	0.4	0.2
Ave.	13.4	12.2	21.0	15.2	4.3
Max.	16.4	15.6	32.7	31.3	10.2
SD	2.3	2.6	5.1	9.7	3.1

$E_C$ : Contour error,  $E_A$ : Area error,  $EFD$ : Ejection fraction difference, SD: Standard deviation.

### C. Discussion

In order to investigate the effects of the NED on the performance of contour extraction, we applied the contour-tracing method directly to the rough contours, i.e., contour candidates without the edges detected by the NED (a weighting factor  $W_W$  was zero) were used. The results of the contour extraction are shown in Table III. The average contour errors of the method with the NED for left ventriculograms at end-diastole and end-systole (6.2% and 17.1%, respectively) were smaller than those of the method without the NED (13.4% and 21.0%, respectively) with statistically significant differences ( $P = 3.06 \times 10^{-8}$  and  $P = 0.0453$ , respectively). The results indicated that the NED contributed to extraction of the contours in agreement with those traced by a cardiologist; in other words, the NED played an important role in making the contours approach those traced by a cardiologist.

Lilly's contour-extraction method [3] is a trainable method which consists of a knowledge-based image transformation, directional gradient search, expectations of object versus background location, least-cost path searches by dynamic programming, and a digital representation of possible versus impossible ventricular shape. Four points (two other points are included in a comparison to the proposed method, i.e., the apical point and a point indicating the extreme position of the mitral valve-inferior wall region) are given to the method manually. According to [3], the method was trained by using 25 images and was tested on 25 images, and an average contour error  $E_C$  of 11.0% and standard deviation of errors of 5.7% were achieved.

Furthermore, we gave consideration to the relationship between the errors of the proposed method and the variability of cardiologists' tracing. The average variation of tracing among cardiologists has been reported: according to [67], the average area error  $E_A$  for the left ventriculograms at end-diastole, that for the left ventriculograms at end-systole, and the average difference of ejection fractions were 7.3%, 15.2%, and 7.0%, respectively. The average area errors for the left ventriculograms at end-diastole and end-systole and the average difference in the ejection fractions of the proposed method were smaller (4.2%, 11.6%, and 4.1%, respectively).

## VI. CONCLUSION

In this paper, we proposed an edge detector based on a multi-layer NN, called an NED, in order to detect the subjective edges that accord with contours traced by a cardiologist, and evaluated a method for extracting LV contours from left ventriculograms by means of the NED. Through experiments with left ventriculograms at end-diastole and at end-systole, it was shown that the

proposed method was able to extract the contours in agreement with those traced by an experienced cardiologist.

In this study, we used the contours traced by a single cardiologist as a “gold standard.” We could use the average contour traced by several cardiologists in order to reduce the bias. We plan to combine the NED with deformable contour models such as Snakes [25] to improve the performance further. We recently investigated the property of the NED in enhancing edges in noisy natural images [68]. We extended the concept of the NED and developed an NN-based scheme for distinction between specific opacities and other opacities in CT images [69].

#### APPENDIX

The NED consists of the modified multilayer NN which employs an identity function instead of a sigmoid function as the activation function of the unit in the output layer. In order to clarify the basic property of the modified multilayer NN with the modified BP algorithm, we considered the relationship between the modified multilayer NN and the original multilayer NN theoretically. As for the structure, we can understand easily that it is difficult for the original multilayer NN to output values near one and zero, whereas the modified multilayer NN can output all values equally. In the modified BP algorithm, the correction of the weight between the unit in the hidden layer and the unit in the output layer is represented by

$$\begin{aligned}\Delta W_m^O &= -\eta \frac{\partial E}{\partial O^O} \frac{\partial O^O}{\partial X} \frac{\partial X}{\partial W_m^O} \\ &= -\eta \frac{\partial E}{\partial O^O} f'_I(X) O_m^H \\ &= -\eta \frac{\partial E}{\partial O^O} O_m^H\end{aligned}\quad (19)$$

where  $O^O$  is the output of the unit in the output layer,  $X$  is the input value to the activation function, and  $f'_I(X)$  is the derivative of an identity function. On the other hand, the correction of the weight in the original BP algorithm is represented by

$$\begin{aligned}\Delta W_m^{OC} &= -\eta \frac{\partial E}{\partial O^O} f'_S(X) O_m^H \\ &= -\eta \frac{\partial E}{\partial O^O} O^O (1 - O^O) O_m^H\end{aligned}\quad (20)$$

where  $f'_S(X)$  is the derivative of a sigmoid function. Comparing the two equations, we find that the difference is just the derivative of the activation function. Therefore, we can rewrite the right side of the above equation as follows, using  $\eta_S$ :

$$-\eta \frac{\partial E}{\partial O^O} O^O (1 - O^O) O_m^H = -\eta_S \frac{\partial E}{\partial O^O} O_m^H.\quad (21)$$

When the training proceeds, the output of the original multilayer NN  $O^O$  should approach the teacher value  $T_C$ . Therefore, the learning rate of the original BP algorithm can be approximated by

$$\eta_S = \eta \cdot O^O (1 - O^O) \approx \eta \cdot T_C (1 - T_C).\quad (22)$$

This equation shows that the learning rate of the original BP algorithm is modulated by the derivative of a sigmoid function, which is 0.5 when the teacher value is 0.5, and is zero when the teacher value is zero or one. In other words, the learning rate of the modified BP algorithm corresponds to that of the original BP algorithm before the modulation. Therefore, in the original BP algorithm, the teacher values of zero and one are never

trained, and the training for the teacher value near zero and one converges more slowly. This would affect the convergence characteristic and the output characteristic. Therefore, the modified multilayer NN with the modified BP algorithm would be suitable for image processing where the teacher values may be continuous values ranging from zero to one, whereas the multilayer NN is suitable for a classification task where the teacher signal is assigned to a class.

#### ACKNOWLEDGMENT

The authors are grateful to K. Koike, K. Ishikawa, and S. Ikeda of Hitachi Medical Corporation for their valuable suggestions, the clinical staffs of Chubu Rosai Hospital for their cooperation, and K. Ueda, of Nagoya Electric Works, Prof. S. Yamamoto, and Prof. S. Okabayashi, of Meijo University for their constructive suggestions. The authors also thank anonymous referees for their helpful suggestions.

#### REFERENCES

- [1] P. Grattani and R. Bonamini, “Contour detection of left ventricular cavity from angiographic images,” *IEEE Trans. Med. Imag.*, vol. MI-4, pp. 72–78, 1985.
- [2] R. E. van Bree, D. L. Pope, and D. L. Parker, “Improving left ventricular border recognition using probability surfaces,” in *Proc. Computers in Cardiology 1988*, 1989, pp. 121–124.
- [3] P. Lilly, J. Jenkins, and P. Bourdillon, “Automatic contour definition on left ventriculograms by image evidence and a multiple template-based model,” *IEEE Trans. Med. Imag.*, vol. 8, pp. 173–185, 1989.
- [4] N. Fan, B. G. Denys, C. C. Li, and P. S. Reddy, “Automated left ventricular border determination in cineangiograms based on a dynamic spider model,” in *Proc. Computers in Cardiology 1990*, 1991, pp. 439–442.
- [5] A. Demi, “New approach to automatic contour detection from image sequences: An application to ventriculographic images,” *Comput. Biomed. Res.*, vol. 27, pp. 157–177, 1994.
- [6] P. Clarysse, D. Friboulet, and I. E. Magnin, “Tracking geometrical descriptors on 3-D deformable surfaces: Application to the left ventricular surface of the heart,” *IEEE Trans. Med. Imag.*, vol. 16, pp. 392–404, Aug. 1997.
- [7] M. Baroni, “Computer evaluation of left ventricular wall motion by means of shape-based tracking and symbolic description,” *Med. Eng. Phys.*, vol. 21, pp. 73–85, 1999.
- [8] M. Moriyama, Y. Sato, H. Naito, M. Hanayama, T. Ueguchi, T. Harada, F. Yoshimoto, and S. Tamura, “Reconstruction of time-varying 3-D left ventricular shape from multiview X-ray cineangiograms,” *IEEE Trans. Med. Imag.*, vol. 21, pp. 773–785, July 2002.
- [9] C. H. Chu, E. J. Delp, and A. J. Buda, “Detecting left ventricular endocardial and epicardial boundaries by digital two-dimensional echocardiography,” *IEEE Trans. Med. Imag.*, vol. 7, pp. 81–90, June 1988.
- [10] P. R. Detmer *et al.*, “Matched filter identification of left-ventricular endocardial borders in transesophageal echocardiograms,” *IEEE Trans. Med. Imag.*, vol. 9, pp. 396–404, Dec. 1990.
- [11] J. Feng, W.-C. Lin, and C.-T. Chen, “Epicardial boundary detection using fuzzy reasoning,” *IEEE Trans. Med. Imag.*, vol. 10, pp. 187–199, June 1991.
- [12] G. Coppini, R. Poli, and G. Valli, “Recovery of the 3-D shape of the left ventricle from echocardiographic images,” *IEEE Trans. Med. Imag.*, vol. 14, pp. 301–317, June 1995.
- [13] I. Mikic, S. Krucinski, and J. D. Thomas, “Segmentation and tracking in echocardiographic sequences: Active contours guided by optical flow estimates,” *IEEE Trans. Med. Imag.*, vol. 17, pp. 274–284, Apr. 1998.
- [14] E. D. Angelini, A. F. Laine, S. Takuma, J. W. Holmes, and S. Homma, “LV volume quantification via spatiotemporal analysis of real-time 3-D echocardiography,” *IEEE Trans. Med. Imag.*, vol. 20, pp. 457–469, June 2001.
- [15] G. Jacob, J. A. Noble, C. Behrenbruch, A. D. Kelion, and A. P. Banning, “A shape-space-based approach to tracking myocardial borders and quantifying regional left-ventricular function applied in echocardiography,” *IEEE Trans. Med. Imag.*, vol. 21, pp. 226–238, Mar. 2002.
- [16] K. P. Philip, E. L. Dove, D. D. McPherson, and K. B. Chandran, “Automatic detection of left ventricular endocardium in cardiac images,” in *Proc. Computers in Cardiology 1990*, 1991, pp. 443–446.

- [17] S. Ranganath, "Contour extraction from cardiac MRI studies using snakes," *IEEE Trans. Med. Imag.*, vol. 14, pp. 328–338, June 1995.
- [18] Y. Zimmer and S. Akselrod, "An automatic contour extraction algorithm for short-axis cardiac magnetic resonance images," *Med. Phys.*, vol. 23, no. 8, pp. 1371–1379, Aug. 1996.
- [19] R. J. van der Geest *et al.*, "Comparison between manual and semiautomated analysis of left ventricular volume parameters from short-axis MR images," *J. Comput. Assist. Tomogr.*, vol. 21, no. 5, pp. 756–765, 1997.
- [20] Y.-P. Wang, Y. Chen, and A. A. Amini, "Fast LV motion estimation using subspace approximation techniques," *IEEE Trans. Med. Imag.*, vol. 20, pp. 499–513, June 2001.
- [21] X. Papademetris, A. J. Sinusas, D. P. Dione, R. T. Constable, and J. S. Duncan, "Estimation of 3-D left ventricular deformation from medical images using biomechanical models," *IEEE Trans. Med. Imag.*, vol. 21, pp. 786–799, July 2002.
- [22] J. S. Duncan, "Knowledge directed left ventricular boundary detection in equilibrium radionuclide angiography," *IEEE Trans. Med. Imag.*, vol. MI-6, pp. 325–336, 1987.
- [23] A. E. Boudraa *et al.*, "Left ventricle automated detection method in gated isotopic ventriculography using fuzzy clustering," *IEEE Trans. Med. Imag.*, vol. 12, pp. 451–465, Sept 1993.
- [24] A. E. Boudraa *et al.*, "Automated detection of the left ventricular region in gated nuclear cardiac imaging," *IEEE Trans. Biomed. Eng.*, vol. 43, pp. 430–437, Apr. 1996.
- [25] M. Kass, A. Witkin, and D. Terzopoulos, "Snakes: Active contour models," *Int. J. Comput. Vis.*, vol. 1, no. 3, pp. 321–331, 1988.
- [26] R. O. Duda and P. E. Hart, *Pattern Classification and Scene Analysis*. New York: Wiley, 1971, pp. 267–272.
- [27] M. H. Hueckel, "A local visual operator which recognizes edges and lines," *J. ACM*, vol. 20, no. 4, pp. 634–647, 1973.
- [28] D. Marr and E. Hildreth, "Theory of edge detection," in *Proc. Royal Soc. London*, vol. B207, 1980, pp. 187–21.
- [29] J. F. Canny, "A computational approach to edge detection," *IEEE Trans. Pattern Anal. Machine Intell.*, vol. PAMI-8, pp. 679–698, 1986.
- [30] W. H. H. J. Lunsher and M. P. Beddoes, "Optimal edge detector design I: Parameter selection and noise effects," *IEEE Trans. Pattern Anal. Machine Intell.*, vol. PAMI-8, pp. 164–177, Mar. 1986.
- [31] M. Petrou and J. Kittler, "Optimal edge detector for ramp edges," *IEEE Trans. Pattern Anal. Machine Intell.*, vol. 13, pp. 483–491, May 1991.
- [32] M. Gudmundsson, E. A. El-kwae, and M. R. Kabuka, "Edge detection in medical images using a genetic algorithm," *IEEE Trans. Med. Imag.*, vol. 17, pp. 469–474, June 1998.
- [33] L. Yin, J. Astola, and Y. Neuvo, "A new class of nonlinear filters - neural filters," *IEEE Trans. Signal Processing*, vol. 41, pp. 1201–1222, Mar. 1993.
- [34] Z. Z. Zhang and N. Ansari, "Structure and properties of generalized adaptive neural filters for signal enhancement," *IEEE Trans. Neural Networks*, vol. 7, pp. 857–868, July 1996.
- [35] L. Yin, J. Astola, and Y. Neuvo, "Adaptive multistage weighted order statistic filters based on the back propagation algorithm," *IEEE Trans. Signal Processing*, vol. 42, pp. 419–422, Feb. 1994.
- [36] K. Suzuki, I. Horiba, and N. Sugie, "Designing the optimal structure of a neural filter," in *Neural Networks for Signal Processing VIII*. Piscataway, NJ: IEEE Press, 1998, pp. 323–332.
- [37] K. Suzuki, I. Horiba, N. Sugie, and M. Nanki, "Noise reduction of medical X-ray image sequences using a neural filter with spatiotemporal inputs," in *Proc. Int. Symp. Noise Reduction for Imaging and Communication Systems*, Nov. 1998, pp. 85–90.
- [38] K. Suzuki, I. Horiba, and N. Sugie, "Signal-preserving training for neural networks for signal processing," in *Proc. IEEE Int. Symp. Intelligent Signal Processing and Communication Systems*, vol. 1, Nov. 2000, pp. 292–297.
- [39] —, "Training under achievement quotient criterion," in *Neural Networks for Signal Processing X*. Piscataway, NJ: IEEE Press, 2000, pp. 537–546.
- [40] —, "Simple unit-pruning with gain-changing training," in *Neural Networks for Signal Processing XI*. Piscataway, NJ: IEEE Press, 2001, pp. 153–162.
- [41] K. Suzuki, I. Horiba, N. Sugie, and M. Nanki, "Neural filter with selection of input features and its application to image quality improvement of medical image sequences," *IEICE Trans. Inform. Syst.*, vol. E85-D, pp. 1710–1718, 2002.
- [42] K. Suzuki, I. Horiba, and N. Sugie, "Efficient approximation of neural filters for removing quantum noise from images," *IEEE Trans. Signal Processing*, vol. 50, pp. 1787–1799, July 2002.
- [43] C. Guzelis and S. Karamahmut, "Recurrent perceptron learning algorithm for CNN's with application to edge detection," in *Proc. IEEE Int. Conf. Image Processing*, 1997, pp. 1134–1139.
- [44] I. N. Aizenberg, N. N. Aizenberg, T. Bregin, C. Butakov, and E. Farberov, "Image processing using cellular neural networks based on multi-valued and universal binary neurons," in *Neural Networks for Signal Processing X*. Piscataway, NJ: IEEE Press, 2000, pp. 557–566.
- [45] I. N. Aizenberg, N. N. Aizenberg, and J. Vandewalle, *Multi-Valued and Universal Binary Neurons—Theory, Learning and Applications*. Boston, MA: Kluwer Academic, 2000.
- [46] H. Nagai, Y. Miyayama, and K. Tochitani, "An edge detection by using self-organization," in *Proc. IEEE ICASSP*, 1998, pp. 2749–2752.
- [47] L. Guan, S. W. Perry, R. Romagnoli, H. Wong, and H. Kong, "Neural vision system and applications in image processing and analysis," in *Proc. IEEE ICASSP*, 1998, pp. 1245–1248.
- [48] P. J. Toivanen, J. Ansamaki, S. Leppajarvi, and J. P. S. Parkkinen, "Edge detection of multispectral images using the 1-D self organizing map," in *Proc. Int. Conf. Artificial Neural Networks*, 1998, pp. 737–742.
- [49] M. S. Bhuiyan, M. Sato, H. Fujimoto, and A. Iwata, "Edge detection by neural network with line process," in *Proc. Int. Joint Conf. Neural Networks*, 1993, pp. 1223–1226.
- [50] H. Iwata, T. Agui, and H. Nagahashi, "Boundary detection of color images using neural networks," in *Proc. IEEE Int. Conf. Neural Networks*, 1995, pp. 1426–1429.
- [51] M. Muneyasu, K. Hotta, and T. Hinamoto, "Image restoration by Hopfield networks considering the line process," in *Proc. IEEE Int. Conf. Neural Networks*, 1995, pp. 1703–1706.
- [52] G. Ohashi, A. Ohya, M. Natori, and M. Nakajima, "Boundary estimation method for ultrasonic 3-D imaging," *Proc. SPIE Medical Imaging, Image Processing*, vol. 1898, pp. 480–486, 1993.
- [53] S. W. Lu and J. Shen, "Artificial neural networks for boundary extraction," in *Proc. IEEE Int. Conf. Systems Man, and Cybernetics*, vol. 3, 1996, pp. 2270–2275.
- [54] Z. He and M. Y. Siyal, "Edge detection with BP neural networks," in *Proc. Int. Conf. Signal Processing*, vol. 2, 1998, pp. 1382–1384.
- [55] K. Suzuki, I. Horiba, K. Ikegaya, and M. Nanki, "Recognition of coronary arterial stenosis using neural network on DSA system," *Syst. Comput. Japan*, vol. 26, no. 8, pp. 66–74, Aug. 1995.
- [56] K. Suzuki, I. Horiba, N. Sugie, and M. Nanki, "Computer-aided diagnosis system for coronary artery stenosis using a neural network," *Proc. SPIE*, vol. 4322, pp. 1771–1782, Feb. 2001.
- [57] K. Funahashi, "On the approximate realization of continuous mappings by neural networks," *Neural Networks*, vol. 2, pp. 183–192, 1989.
- [58] A. R. Barron, "Universal approximation bounds for superpositions of a sigmoidal function," *IEEE Trans. Inform. Theory*, vol. 39, pp. 930–945, Mar. 1993.
- [59] D. E. Rumelhart, G. E. Hinton, and R. J. Williams, "Learning representations of back-propagation errors," *Nature*, vol. 323, pp. 533–536, 1986.
- [60] —, "Learning Internal Representations by Error Propagation," in *Parallel Distributed Processing*. Cambridge, MA: MIT Press, 1986, vol. 1, ch. 8, pp. 318–362.
- [61] N. Otsu, "A threshold selection method from gray-level histograms," *IEEE Trans. Syst. Man, Cybern.*, vol. SMC-9, pp. 62–66, Jan. 1979.
- [62] A. V. Oppenheim and R. W. Schaffer, *Digital Signal Processing*. Englewood Cliffs, NJ: Prentice-Hall, 1975.
- [63] G. B. Trobaugh, A. P. Hallstrom, and J. W. Kennedy, "Reproducibility of ventricular function measurements by contrast angiography," *Catheterizat. Cardiovasc. Diagnosis*, vol. 10, no. 6, pp. 561–572, 1984.
- [64] K. Suzuki, I. Horiba, and N. Sugie, "A simple neural network pruning algorithm with application to filter synthesis," *Neural Processing Lett.*, vol. 13, no. 1, pp. 43–53, Feb. 2001.
- [65] C. Schaffer, "Selecting a classification method by cross-validation," in *Proc. 4th Int. Workshop Artificial Intelligence and Statistics*, Jan. 1993, pp. 15–25.
- [66] K. Suzuki, I. Horiba, and N. Sugie, "Linear-time connected-component labeling based on sequential local operations," *Comput. Vis. Image Understanding*, vol. 85, no. 1, pp. 1–23, Jan. 2003.
- [67] P. F. Cohn, J. A. Levin, G. A. Bergeron, and R. Gorlin, "Reproducibility of the angiographic left ventricular ejection fraction in patients with coronary artery disease," *Amer. Heart J.*, vol. 88, pp. 713–720, 1974.
- [68] K. Suzuki, I. Horiba, and N. Sugie, "Neural edge enhancer for supervised edge enhancement from noisy images," *IEEE Trans. Pattern Anal. Machine Intell.*, vol. 25, pp. 1582–1596, Dec. 2003.
- [69] K. Suzuki, S. G. Armato, III, F. Li, S. Sone, and K. Doi, "Massive training artificial neural network (MTANN) for reduction of false positives in computerized detection of lung nodules in low-dose CT," *Med. Phys.*, vol. 30, no. 7, pp. 1602–1617, July 2003.